An optimal energy management strategy for a photovoltaic/li-ion battery power system for DC microgrid application

Salam J. Yaqoob[1]*, Husam Arnoos[2], Mohammed A. Qasim[3,4], Ephraim B. Agyekum[3], Ahmad Alzahrani[5]* and Salah Kamel[6,7]*

[1]Department of Research and Education, Authority of the Popular Crowd, Baghdad, Iraq, [2]Department of Control and Communication, The Ministry of Electricity, Baghdad, Iraq, [3]Nuclear Power Plants and Renewable Energy Sources Department, Ural Federal University, Yekaterinburg, Russia, [4]Department of Projects and Engineering Services, Ministry of Health, Baghdad, Iraq, [5]Electrical Engineering Department, College of Engineering, Najran University, Najran, Saudi Arabia, [6]Electrical Engineering Department, Faculty of Engineering, Aswan University, Aswan, Egypt, [7]Applied Science Research Center, Applied Science Private University, Amman, Jordan

The purpose of this paper is to propose an energy management strategy (EMS) based on flatness control method for a standalone hybrid photovoltaic-battery system. The goal of the proposed method is to use non-linear flatness theory to develop an efficient EMS in order to provide a stable DC bus voltage and an optimal power sharing process between the solar array and the battery. The suggested EMS is responsible for balancing the power reference for the PV system and the battery while keeping the DC bus voltage steady and performing at its reference value. In order to maximize the PV's power, a perturb and observe with a variable step size (VSSP and P&O) based maximum power point tracking (MPPT) method with a DC/DC boost converter was used. In addition, a DC/DC bidirectional converter was developed to control the charging and discharging process of the battery. Moreover, the proposed EMS strategy was verified in a MATLAB®/Simulink-based simulation environment by subjecting it to a variety of scenarios, including those with varying degrees of irradiation and sudden changes in load. The obtained results show that the presented EMS method was able to keep the bus voltage stable despite changes in load or solar radiation. Furthermore, the EMS By minimizing bus voltage spikes, the technique also ensured excellent power quality which helped the battery's operation in terms of lifetime and efficiency. Finally, the suggested strategy has a minimum overshoot rate in the bus voltage and higher tracking efficiency compared with the classical load following (LF) strategy under various load conditions.

KEYWORDS

energy management system, lithium battery, photovoltaic, hybrid power system, flatness, boost converter, modified P&O

1 Introduction

1.1 Background and motivation

Microgrid (MG) operation with distributed generation units (DG) and renewable energy sources (RES), such as photovoltaic (PV) systems, wind turbine (WT), and proton exchange membrane (PEM) fuel cells (FC), is now the most commonly used in electrical power systems (Evans et al., 2009; Qazi et al., 2019; Sinsel et al., 2020). In addition, the use of these sources necessitates the addition of a supplementary energy storage system unit in order to reduce

power fluctuations and increase the availability of electricity (Molina and Juanico, 2010). In contrast, stand-alone or off-grid photovoltaic (PV) systems using Li-ion batteries that are more efficient have gained popularity in recent years (Vonsien and Madlener, 2020). It is essential in that system to have an EMS between the photovoltaic cells, the battery, and the load in order to transfer the right amount of power between the sources and increase the lifespan of the battery (Rydh and Sandén, 2005; Bragard et al., 2010; Campana et al., 2021). In point of fact, it is possible to achieve the maximum power of the PV system by using a maximum power point tracking (MPPT) device. This device not only improves the effectiveness of the PV systems but also improves their performance in a variety of weather conditions (Saleh et al., 2020; Yaqoob et al., 2020). In order to manage the duty cycle and extract the peak power, an MPPT device is installed into a PV system or module with an appropriate DC/DC converter. Several other MPPT methods, including perturb and observe (P & O), incremental conductance (IC), fuzzy logic, and several others, are used in the application of PV systems (Rizzo and Scelba, 2015; Robles Algarín et al., 2017; Rezk et al., 2019; Shang et al., 2020). Managing lithium-ion batteries, on the other hand, can improve performance, extend battery life, and cut down on power losses in the grid. The right way to manage the battery may help keep the DC bus voltage constant and improve the way power is shared between the load and the generator (Mesbahi et al., 2017; Hannan et al., 2018; Berrueta et al., 2020).

1.2 Previous works

Off-grid photovoltaic (PV) systems or DCMG systems with battery energy storage systems and renewable energy sources have been proposed by a number of researchers (Shiau et al., 2009; Ongaro et al., 2012; Li et al., 2015). These systems are intended to improve efficiency and deliver optimal power to the load by utilizing power DC/DC converters. For example, the authors of (Fathabadi, 2019) proposed a hybrid power system consisting of solar panels, fuel cells, and batteries that could charge electric vehicles (EVs) that use lithium-ion batteries. The work that was given was modeled and simulated by utilizing the MATLAB® and Simulink software, and the efficiency of the system fulfilled expectations. This was shown by the fact that the generated outputs matched up with the outcomes that were needed. It was also found out that it is feasible to increase the energy efficiency of this system by making use of electrical equipment that is more energy efficient, such as batteries that run on lithium-ion. In a remote location, Khadepaun et al. (Khadepaun and Shah, 2020) presented a demonstration of a hybrid MG that was powered by a solar PV system as well as PEMFC cells. According to the findings of this research, the use of environmentally friendly fuel cells as energy source units in small grid plants is the superior choice to the utilization of lithium batteries, which have a life span of between five and 7 years. When it has reached the end of its useful life, it should be thrown away, which is another way in which it harms the environment. According to the findings of the research, making use of DC loads, such as electric vehicles, lights, and chargers, makes the MG system more efficient and productive since it eliminates losses that would have been generated by shifting current from DC to AC. The power system that Gonzalez et al. (Gonzalez et al., 2019) suggest using is a PV/FC/battery MG system that also includes a battery unit for energy storage. The model predictive control method is used inside an EMS in order to

distribute the appropriate amount of real power to the grid. This strategy cuts down on how much power the battery needs, but it depends on how accurate the prediction is, which is a variable and unpredictable factor.

The authors of (Tofighi and Kalantar, 2011) suggested using EMS to manage the power flow between the sources and load for a PV/battery system using linear PI management. This would allow the authors to control the flow of power. MATLAB® and Simulink were used in order to verify the accuracy of the provided technique. The findings that were acquired were achieved under a variety of load situations, and they demonstrate that the suggested PV-battery system has a quick speed response as well as a minimal oscillation in DC voltage. However, in classic EMS, a proportional-integral (PI) control was used to regulate the power sharing between PV, the battery, and the load (Kewat et al., 2018). This type of control has several problems, the most important of which are the need for tuning, the linear control type, and the slow dynamics.

The study in (Sharma et al., 2022) presented a sensitivity analysis and techno-economic modeling of a MG system consisting of solar, wind, hydro, and battery storage, with this MG system linked to the utility grid. One benefit of the on-grid approach for rural areas is that any extra power from RES can be sold back to the utility grid. This helps find the lowest Levelized Cost of Energy (LCOE) and Total Net Present Cost (TNPC). The authors in (Belaid et al., 2022a; Belaid et al., 2022b), proposed a power management control (PMC) based optimization for a wind/battery system. This method is created and coupled to the suggested two-level MPPT controller in order to facilitate the management of the wind and battery power system. The used PMC guarantees that the utilised storage batteries are subjected to the least amount of stress possible by providing efficient optimum functioning of two MPPT algorithms. The primary purpose of the PMC-based system is to meet the power requirements of the load, while secondary goals include preserving the state of charge of the battery bank, avoiding power outages, and maximizing the useful life of the batteries. The authors in (Dashtdar et al., 2022) proposed an EMS for a residential MG system in order to reduce the cost of operating the MG sources. The suggested EMS method is implemented on the combined heat power (CHP) with batteries and the obtained results show the effect of the battery on MG participation in load response. In addition, the cost of operating a MG and how to exchange with the grid under varying market price tariffs are analyzed, with results demonstrating the efficacy of the suggested strategy.

1.3 Research contributions

This article presents an optimum EMS based on the non-linear flatness control theory for an off-grid hybrid solar PV system.

The following are the main contributions that are presented by this research:

1 Suggests a non-linear control based EMS for PV-battery power systems that provides excellent quality for the output power.
2 Manages the Li-ion battery based on its power reference in order to ensure optimal performance and stable voltage at the DC link connection.
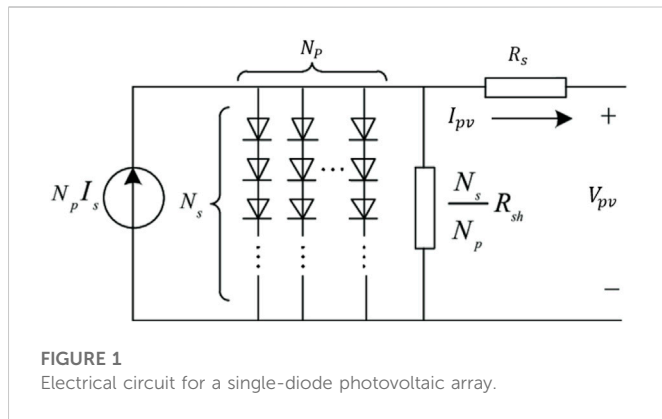
FIGURE 1
Electrical circuit for a single-diode photovoltaic array.

TABLE 1 Datasheet parameters of the KC200GT PV module at STC conditions.

Parameter	Value
P_{mpp}	$200\,W$
V_{oc}	$32.9\,V$
V_{mpp}	$26.3\,V$
I_{sc}	$8.21\,A$
I_{mpp}	$7.61\,A$
K_i	$0.00318\,A/K$
K_v	$-0.123\,V/K$
N_{ser}	54

3 Proposes a highly efficient VSSP&O based MPPT to optimize the output power of the PV array without power oscillation.

1.4 Research structure

This paper was structured into the following sections: Section 2 introduces photovoltaic system modeling. Section 3 presents the proposed energy management strategy. Section 4 reports the simulation results and discussion. Finally, Section 5 presents the conclusion of the paper.

2 Photovoltaic system modeling

2.1 Model of PV array

Figure 1 depicts the electrical circuit of a PV cell model used in this study (Molina and Juanico, 2010; Saleh et al., 2020). It is simple and straightforward to express in the MATLAB® environment and provides enough representation for the PV array. The PV array current (I_{pv}) for given $N_P \times N_s$ can be written as follows (Molina and Juanico, 2010).

$$I_{pv} = N_P I_s - N_P I_o \left[exp\left(\frac{V_{pv} + R_s\left(\frac{N_S}{N_P}\right).I_{pv}}{\gamma V_{Th} N_S} \right) - 1 \right] - \frac{V_{pv} + R_s\left(\frac{N_S}{N_S}\right).I_{pv}}{R_{sh}\left(\frac{N_S}{N_P}\right)}$$

(1)

where the components in the above equation are summarized as follows:

  ✓I_{Ph} is the source of the photo.
  ✓I_o is the current of diode *via* a saturation case
  ✓V_{pv} is the array's voltage
  ✓R_s is the series resistance
  ✓R_{sh} is the parallel resistance
  ✓N_S is the total number of panels in a sequence.
  ✓N_P is the number of parallel panels
  ✓γ is the constant of the diode
  ✓V_{Th} is the thermal voltage $V_{th} = N_{ser}KT/q$.
  ✓N_{ser} is the total number cells for one a PV module
  ✓T is the temperature
  ✓K is the constant of Boltzmann (1.3806503×10^{-23} J/°K)

FIGURE 2
Block diagram of the suggested MPPT controller with boots converter.

  ✓q is the charge value of the electron ($1.60217646 \times 10^{-19}$C).

Furthermore, in this research, the PV array employed in simulation is made up of 5×10 array, resulting in a large PV array of 10 kW to deliver adequate DC power and voltage to the DC load side and battery. Furthermore, the employed PV array was connected *via* a DC/DC boost converter to amplify the PV voltage and implement the MPPT algorithm for varied irradiance profiles. Table 1 shows the datasheet parameters of the employed PV module type KC200GT under STC circumstances (Energy Matters, 2020). These parameters include maximum output power P_{mpp} , the voltage of the open-circuit V_{oc} , the voltage at MPP V_{mpp} , current at MPP I_{mpp} , short-circuit current I_{sc} , temperature coefficient at I_{sc} (K_i) , temperature coefficient at V_{oc} (K_v) and N_{ser} .

2.2 Suggested MPPT method

A MPPT approach is required in PV system applications to optimize power from the PV system and to increase system performance under varying weather conditions (Rizzo and Scelba, 2015; Yaqoob et al., 2020). Furthermore, the MPPT control is used to create the required duty cycle and to activate the boost circuit's switch as seen in Figure 2. Several low-cost and easy MPPT approaches, including P&O and IC techniques, were applied to extract the maximum power from the PV module (Saleh et al.,
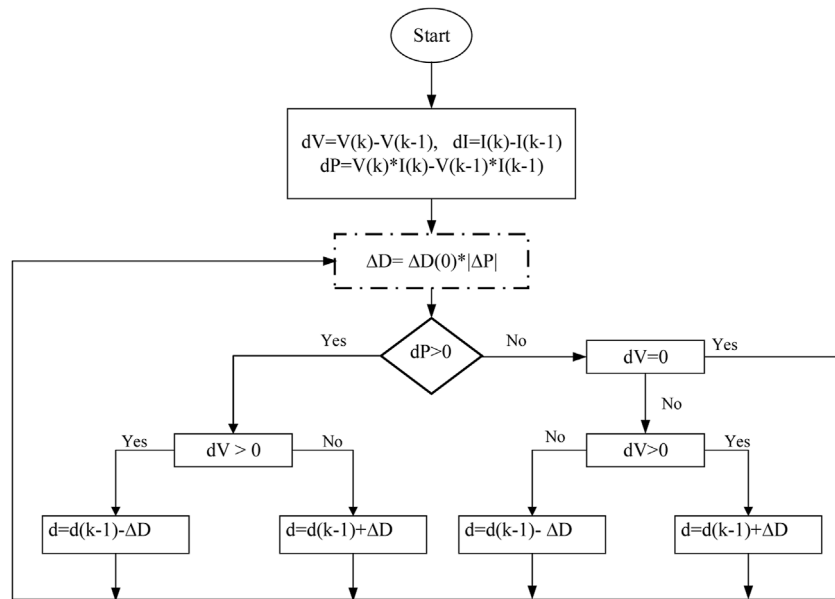
FIGURE 3
Flowchart of the modified VSSP&O MPPT technique.
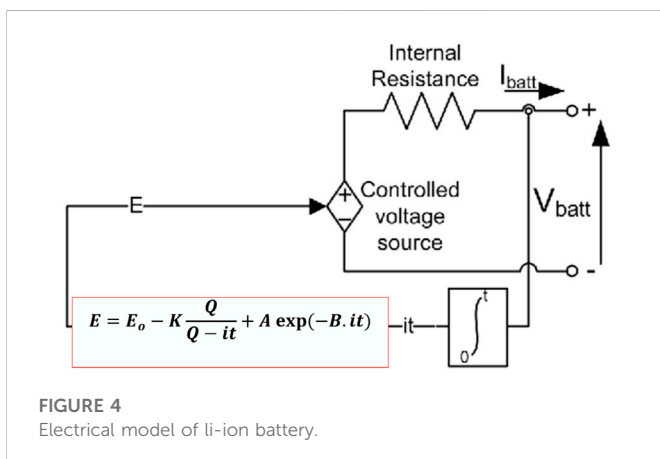
FIGURE 4
Electrical model of li-ion battery.

TABLE 2 The battery's design parameters.

Description	Value
V_b	48 V
Q	50 Ah
E_0	52.04 V
K	0.007192
R_b	0.0096 Ω
A_b	4.03 V
B	1.22 Ah^{-1}

2020; Yaqoob et al., 2020). In this paper, a VSSP&O MPPT was used to track the MPP of the P-V characteristics of the PV system. The flowchart of the presented MPPT method is illustrated in Figure 3. The presented MPPT was designed with a variable step size in order to vary the duty ratio with respect to the change in power. Thus, this method is more efficient than the traditional fixed step size P&O. Therefore, the PV system will be controlled without power oscillation around the MPP, and the performance will be improved.

2.3 Li-ion battery modeling

Li-ion batteries are extensively used in many power systems due to their increased efficiency when compared to other technologies (Ferahtia et al., 2021). It is known as a lithium-metal battery because it contains metallic lithium as an anode. However, a

greater energy density was attained from a battery with a little power density. The increased energy density of the Li-ion battery makes it more appropriate for off-grid PV applications, especially when electricity availability is limited. The battery model utilized in this study is based on the MATLAB/Simulink® model shown in Figure 4. The battery's output voltage can be stated as follows (Ferahtia et al., 2021):

$$V_b = E_0 - K \frac{Q}{Q - i_t} - R_b i + A_b e^{(-Bi_t)} - K \frac{Q}{Q - i_t} i^\star \quad (2)$$

where the above battery's parameters can be defined as.

- V_b is the output voltage of the battery (V),
- E_0 is the voltage at the open-circuit case
- Q is the normal battery's capacity (Ah),
- K is the polarization constant,
- it is the current battery charge ($it = \int idt$) (Ah).
- A_b denotes the exponential zone amplitude (V);
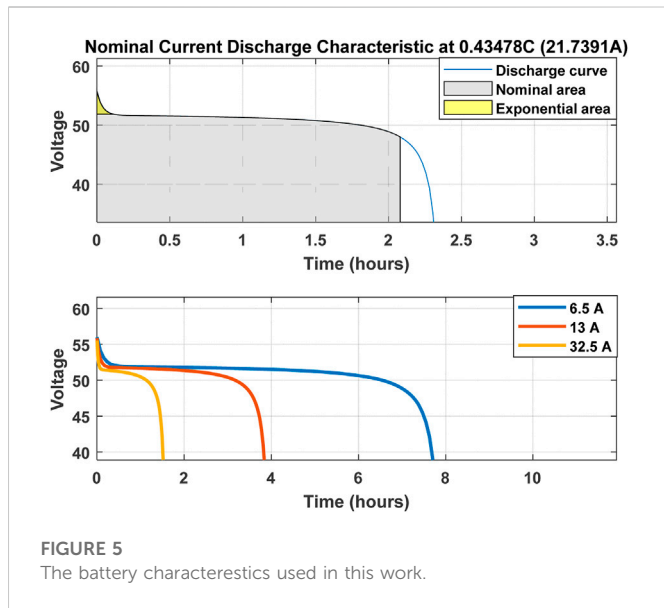
FIGURE 5
The battery characterestics used in this work.

- B denotes the exponential zonetime constant inverse in the exponential zone (Ah^{-1});
- R_b is the internal resistance (Ω), and
- i and i^* are the battery current and the filtered current (A), respectively.

The battery design was implemented under simulation based on the characteristics listed in Table 2. The battery module parameters are shown in Figure 5. The initial SOC of the battery is 95%. A battery bank of 50 Ah with a voltage of 48 V was used in this study. The maximum extracted energy from the battery is 2,400 Wh, and this value can cover the demnded load that used in this analysis.

2.4 Desing of boost converter

The electrical boost converter circuit that shown in Figure 2 have three main parameters which are should be calculated to design the boost conveter in the simulation or practical operation. As a result, the following Equations 3-5 are utilized for the inductor current (L), the input capacitor (C_{in}), and the output capacitor (C_{out}) (Saleh et al., 2020):

$$L = \frac{V_{pv}\,\delta}{f_s \Delta I_{pv}} \tag{3}$$

$$C_{in} \geq \frac{\delta}{8 \times f_s^2 \times L \times 0.01} \tag{4}$$

$$C_{out} = \frac{I_{out}\,\delta}{f_s \Delta V_{out}} \tag{5}$$

where V_{out} represents the voltage of the boost converter, the volatge's ripple denotes by $\Delta V_{out} = 0.02 V_{out}$, δ is the duty cycle, f_s is the switching frequency, and the ripple in the inductor current is $\Delta I_{pv} = 0.3 I_{pv}$. In this study, the continuous conduction mode (CCM) was used to analyze boost circuit and compute the electrical parameters of the circuit. By assuming the maximum duty ratio is 0.8, the inductance, the input capacitor, and the output capacitor are $1\,mH$, $600\,\mu F$, and $1000\,\mu F$, respectively.

3 Proposed EMS strategy

Using a PV-Li-ion battery as a hybrid power system, as seen in Figure 6, can improve the performance and meet the load demand. As seen in Figure 1, both a Li-ion battery and a PV system are connected to the DC bus by a DC/DC boost converter and a bidirectional DC/DC converter, respectively, to supply the DC load. In this study, an efficient EMS based on flatness control theory is utilized to estimate the reference power of the battery and supply the DC load demand while maintaining the bus voltage within standard limits $(V_{bus} = 380V)$.

Because of the system's non-linearity for the PV-battery system, the control technique may be more complicated. Because of this, the classical linear PI control method was replaced with the differential non-linear flatness theory to reduce the order of the model (Ferahtia et al., 2020):

$$y = \phi\left(x, u, \dot{u}, \ldots u^{(\alpha)}\right) \tag{6}$$

$$x = \varphi\left(y, \dot{y}, \ldots y^{(\beta)}\right) \tag{7}$$

$$u = \psi\left(y, \dot{y}, \ldots y^{(\beta+1)}\right) \tag{8}$$

where the above items can be indicted below:

- y is the flat model,
- x is the state variable,
- u is the control variable,
- ψ are the functions of the smooth mapping,
- $y^{(\beta+1)}$ is the notation for the derivative of the output $(\beta+1)^{th}$.
- Also, α is a finite number of the derivative, while
- $(\phi) = m$, $rank(\varphi) = n$, and $rank(\psi) = m$ (Ferahtia et al., 2020).

The proposed EMS was applied to the HPS system to estimate the required power from the load and generate the optimal EMS for the battery and the PV system. The proposed model under flatness theory was defined as follows:

$$x = \sqrt{2y/C_{bus}} = \phi(y) \tag{9}$$
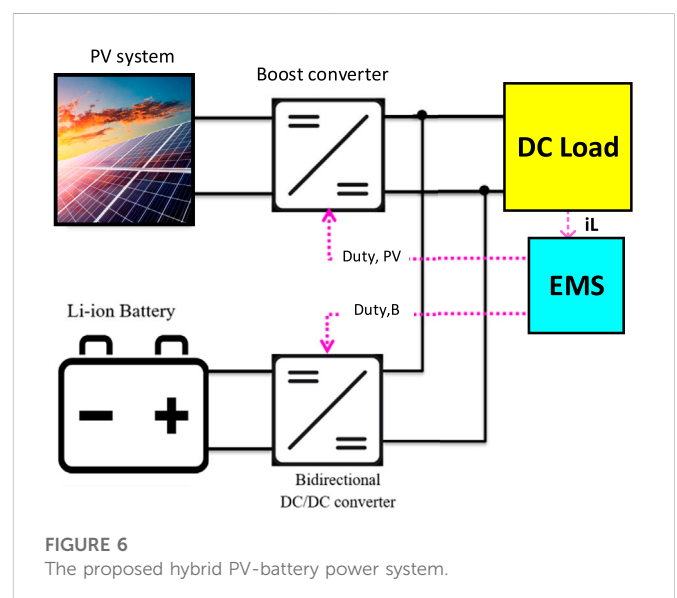
FIGURE 6
The proposed hybrid PV-battery power system.
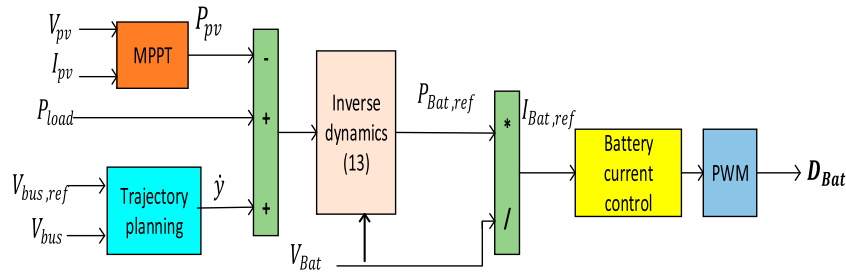
FIGURE 7
Proposed EMS of the hybrid PV-battery model.

$$y_{bus} = \frac{1}{2} C_{bus} v_{bus}^2 \qquad (10)$$

where C_{bus} is the DC bus capacitance, and v_{bus} is the bus voltage. Based on the proposed system configuration, the bus energy y_{bus} can be written as a function of the power-sharing through the DC bus (Ferahtia et al., 2020):

$$\dot{y}_{bus} = P_{PVo} + P_{Bato} - P_{load} \qquad (11)$$

where P_{PVo} and P_{Bato} are the generated power from the PV system and battery, including switching converter losses, respectively.

$$P_{PVo} = P_{PV} - r_{PV}\left(\frac{P_{PV}}{v_{PV}}\right)^2 \qquad (12)$$

$$P_{Bato} = P_{Bat} - r_{Bat}\left(\frac{P_{Bat}}{v_{Bat}}\right)^2 \qquad (13)$$

where r_{PV} and r_{Bat} are the PV converter losses and battery converter losses, respectively.

Furthermore, both the PV and battery follow their power reference values, which are expressed in Eqs 15, 16. The output power of the PV system was tracked using an MPPT controller, while the power of the battery module was estimated using trajectory planning in flatness control.

$$P_{Bat\_ref} = P_B = v_B\, i_B \qquad (14)$$

$$P_{PV\_ref} = P_{PV} = v_{PV}\, i_{PV} \qquad (15)$$

Furthermore, the input control unit (u) represents the battery power reference expressed from Eqs 9–15 as,

$$u = P_{Bat,ref} = 2P_{Bat,max}\left[1 - \sqrt{1 - \sqrt{\frac{\dot{y} + \sqrt{\frac{2y}{C_{bus}}} \cdot i_{load} - P_{PVo}}{P_{Bat,max}}}}\right]$$

$$= \psi\left(\dot{y}, y\right) \qquad (16)$$

where is the limited maximum power of the battery, $P_{Bat,max} = \frac{v_{Bat}^2}{4\, r_{Bat}}$.

Moreover, the most critical variable in the proposed system is the flat output = y_{bus}. So, to make this flat controllable, a PI controller is applied to ensure and regulate the dc bus voltage. Actually, the SC control loop is considered faster than the battery. As a result, the overall power of the HPS in Eq. 11 can be written as

$$\dot{y}_{bus} = P_{Bato} \qquad (17)$$

TABLE 3 Simulation parameters of the system.

Item	Value
v_{bus}	$380\,V$
v_b	$48\,V$
C_{bus}	$1000\,\mu F$
K_p	2500
K_i	60
ω_n	50
ζ	0.6
r_{PV}	0.01
r_{Bat}	0.01

From this equation, it is clear that the output transfer function is a pure integrator. So, a PI controller is applied based on the supposing of $y_{ref} = y_{bus,ref}$, the following control equation of DC bus voltage low is expressed as (Ferahtia et al., 2020),

$$\dot{y} = \frac{1}{s}\left(K_p + \frac{K_i}{s}\right)\left(y - y_{ref}\right) \qquad (18)$$

where $K_p = 2\,.\zeta.\omega_n$, $K_i = \omega_n^2$, ω_n is the natural frequency and ζ is the damping factor.

The block diagram of the proposed EMS is illustrated in Figure 7.

4 Simulation results and discussion

Following the design of the control strategy, MATLAB/Simulink®2021 software was used to test and prove the hybrid power system in order to validate the effetiveness of the proposed EMS. Both the PV system and the battery are connected to a shared DC bus *via* DC/DC converters, and the control system is employed to keep the voltage constant at its reference. The reference voltage for the DC bus is 380V, which is tracked to ensure stability. The parameters of the proposed system are listed in Table 3.

Moreover, the proposed HPS was tested at different irradiance profiles. To emulate the real irradiance variations, the irradiance profile shown in Figure 8 was utilized to demonstrate the system's
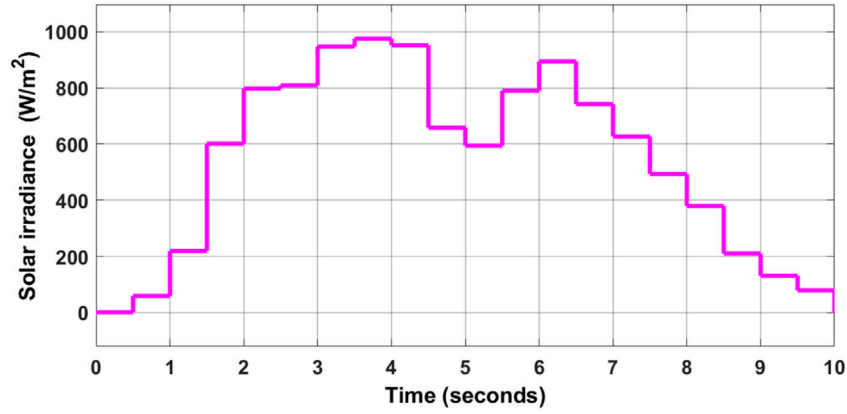
FIGURE 8
The solar irradiance profile used in this study.
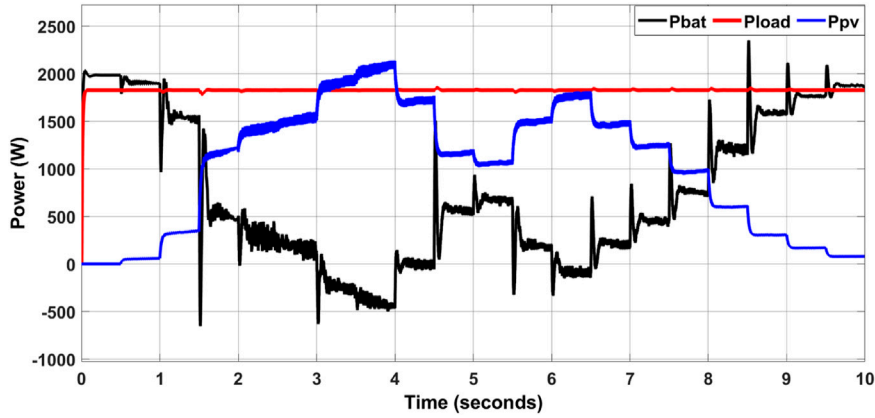
FIGURE 9
Power graphs of the PV system, load, and battery.
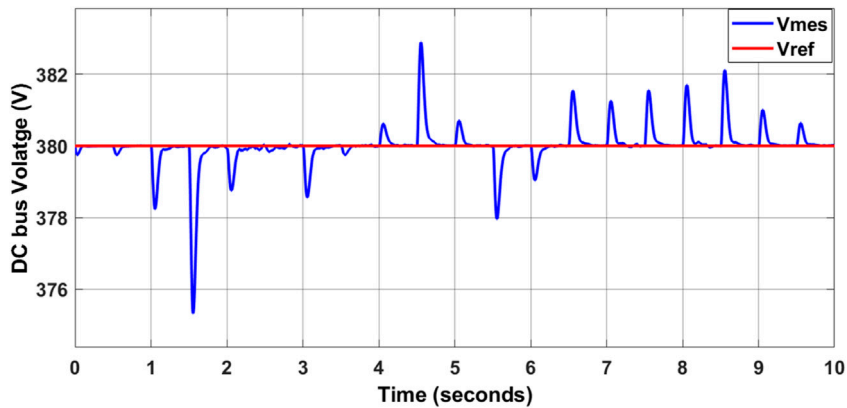
FIGURE 10
Simulation result of DC bus voltage.

performance. The temperature is assumed to be 25℃. A step in solar irradiation is applied during the simulation time of 10 seconds, ranging from 0 to $1000 W/m^2$. Therefore, the PV power will increase by increasing the irradiance level, as seen in Figure 9. As seen in Figure 9, in the initial case, the demand load is fixed from the time of $t = 0 sec$ to $= 1 sec$. At this moment, the
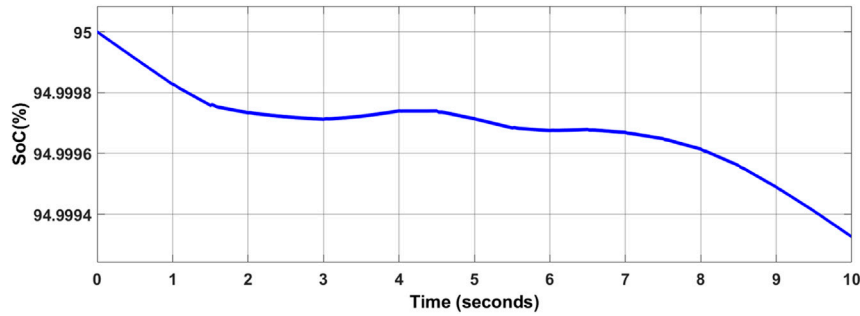
FIGURE 11
SOC of the battery.
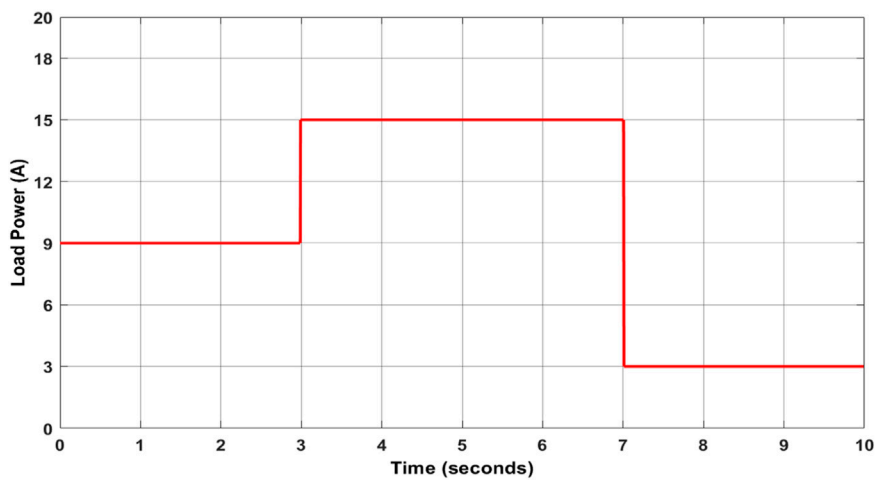
FIGURE 12
The suggested load profile.

demand load is supplied by the battery due to the generation from the PV system being small. It is clear that the PV power is less than the demand; as a result, the battery begins to supply the required power. After a time interval of $= 2\,sec$, either the PV system or the battery will supply the demand DC load depending on the irradiance levels, so the battery may absorb the additional power or supply the load with the needed power throughout the simulation.

The results of the DC bus voltage during 10 s are shown in Figure 10. The first curve which is drawn in red colour represents the DC bus reference voltage, while the second curve in blue represents the measuring DC bus voltage under varying irradiance levels. As a result of this, the DC bus voltage utilizing the proposed EMS can provide improved performance with faster response and less overshoot, as well as more resilience. Furthermore, the DC bus voltage is stabilized, with a maximum overshoot voltage of $6\,V$ (1.3%). Also, the voltage ripple is reduced by means of an efficient EMS ($\Delta V = 4.5\,V$).

The state of charge (SOC) of the battery is illustrated in Figure 11. As seen, this figure explains the behavior of the Li-ion battery. It mainly supplies (discharges) with a decrease in solar irradiance. While it charges (absorbs) with the step-up in irradiance.

To validate the performance of the proposed EMS, the DC load power profile shown in Figure 12 is used. In this case, the output power of the PV system is extracted with constant weather conditions of $G = 1000W/m^2$ and $T = 25\,℃$ while the load is varied during the simulation.

Figure 13 reports power curves that were obtained during the simulation. This figure shows the battery power, load power, and PV system power. In the initial simulation, the power of the load is relatively high (3400 W) while the extracted power from the PV system is smaller than the demand load (2650 W); as a result, the battery begins supplying the needed power.

Furthermore, at $t = 3\,sec$, the load power jumps from 3400 W to 5700 W, requiring the battery to supply practically all of the transient load because the demand exceeds the generating power from the PV system.

At $= 7\,sec$, the load power decreases (from 5700W to 1150W). The following observations are made:

- The Li-ion battery absorbs the surplus of the bus power with limited power dynamics.
- The PV system supplied the demand power
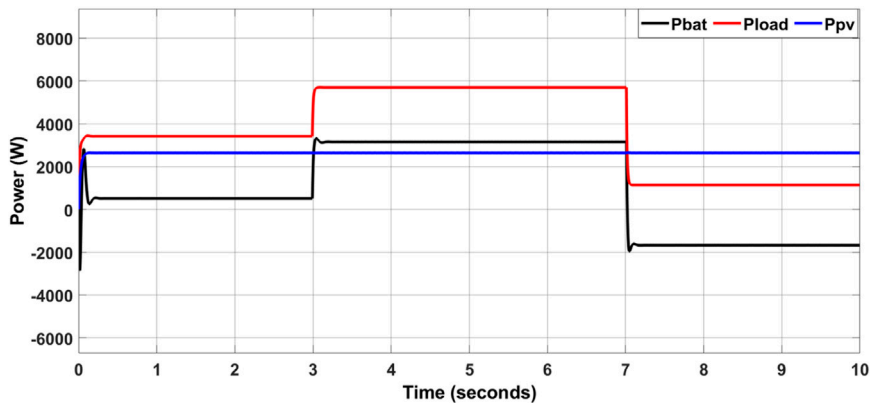
FIGURE 13
Power curves of the PV system, load and battery.
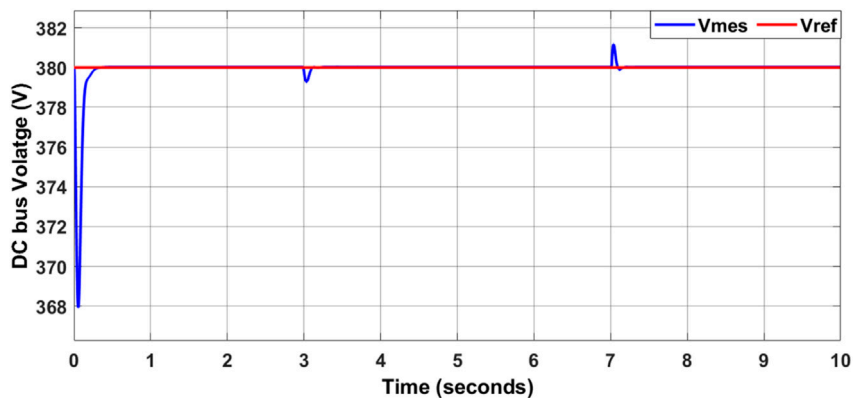
FIGURE 14
Simulation result of DC bus voltage.
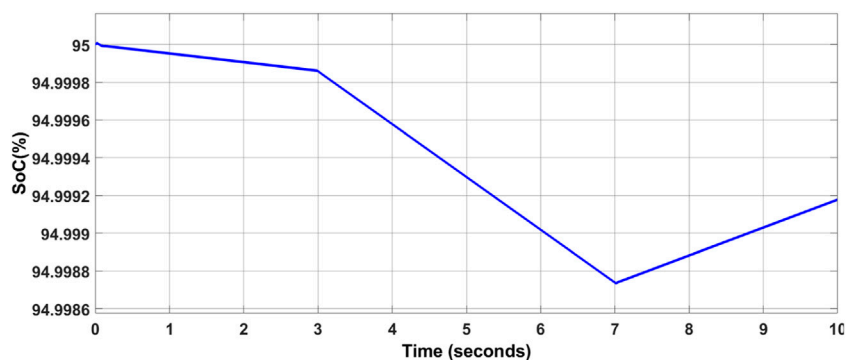
FIGURE 15
SOC of the battery under various values of the load.

The proposed EMS successfully controls the voltage of the DC bus, as seen in Figure 14 in the case of different load conditions. This figure demonstrates the effectiveness of the proposed EMS in achieving DC bus voltage stability and minimizing ripple content while maintaining excellent power quality. Figure 15 shows the SOC of the battery in the case of varying load power conditions.
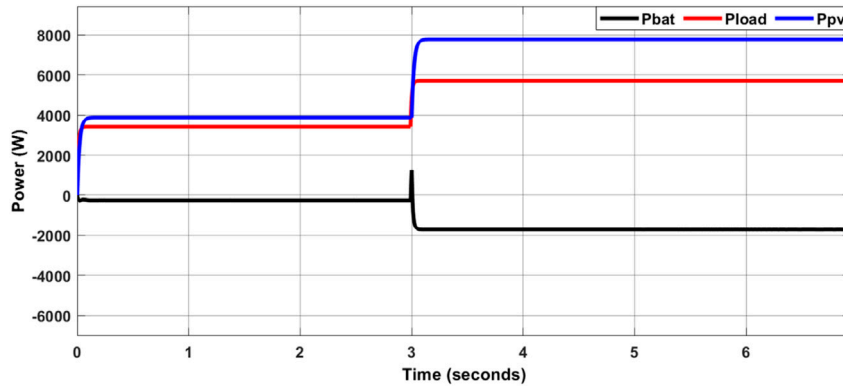
FIGURE 16
Power curves of the PV system, load and battery with changes in both PV and load.
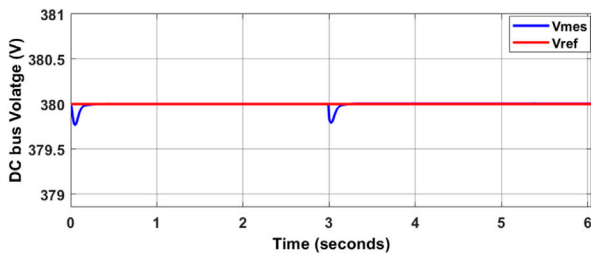
FIGURE 17
The obtained result of the DC bus voltage under various irradiance and load conditions.

In order to include more results with changes in both PV and load at the same time, Figure 16 reports power curves that were obtained for step changes in irradiance and output load. As seen in this figure, in beginning the PV system supplied the demand load while keeping the battery in charging mode according to its SOC. When the power system is subject to a fast change in PV generation and a high transient load, the PV power provides the increase in the load and the excess energy is used to charge the battery. As can be observed in Figure 17, the voltage of the DC bus is successfully controlled by the EMS that has been proposed, even when

subjected to a variety of load and irradiance. This figure indicates that the suggested EMS is effective in attaining DC bus voltage stability. Figure 18 illustrates the SOC of the battery under a variety of load power and irradaiton circumstances.

To prove the novelty of the suggested EMS, a comparison between the proposed EMS and the conventional load following (LF) based EMS strategy under different load conditions was presented as seen in Table 4. It is clear that the suggested strategy has a minimum overshoot rate in bus voltage and higher tracking efficiency compared with the classical LF strategy.

In summary, the optimal EMS of the Li-ion battery will extend its lifetime, which is an important issue in a hybrid PV-battery system. Furthermore, stabilizing the DC bus voltage with its reference value allows the system to run at high power quality.

5 Conclusion and future work

In this research, an optimal energy management strategy (EMS) for a hybrid PV-battery system-based on non-linear flatness theory was presented. First, the mathematical analysis with details for both the PV array and Li-ion battery was presented. Second, the non-linear flatness theory was derived and applied to the proposed PV-battery system to estimate the desired power for the PV system and battery. MATLAB/
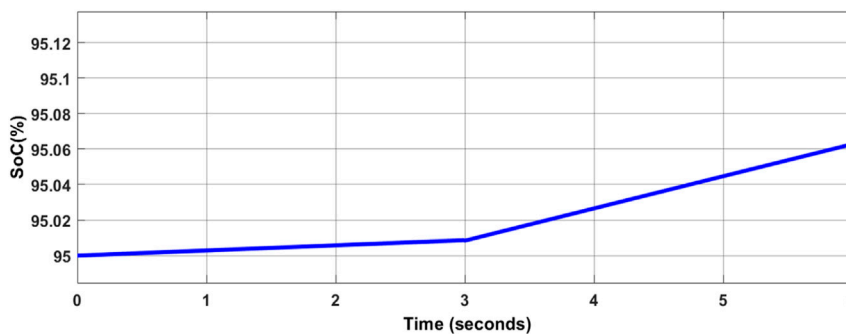
FIGURE 18
SOC of the battery.

TABLE 4 Comparison between the proposed EMS and the conventional LF method under different load conditions.

Change in load power (W)	Conventional LF		Proposed EMS	
	Overshoot in V_{bus} (V)	Tracking efficiency (%)	Overshoot in V_{bus} (V)	Tracking efficieny (%)
$170 \rightarrow 190$	6	97	0.73	99.4
$190 \rightarrow 900$	10	98	1.33	98.1
$900 \rightarrow 1300$	7	98.4	1.22	98.8
$1300 \rightarrow 2000$	6.5	98	1.2	98.4
$2000 \rightarrow 2100$	2	98.7	0.8	99

Simulink® was used to model and simulate the proposed EMS. The performance of the proposed system was tested under both irradiance and load power variations. According to the simulation findings, the suggested EMS provides high power quality by stabilizing the values of the DC bus voltage and providing low ripple content in bus voltage ($\Delta V = 4.5\,V$) as well as a minimum value of maximum overshoot in voltage (1.3 %).

This study recommends the following topics for further research: 1) analysis of the flatness EMS with a new DC MG containing FC, PV, and supercapacitor module; and 2) design and implementation of a new EMS with an online optimization approach-based MG system.

Data availability statement

The original contributions presented in the study are included in the article/supplementary material, further inquiries can be directed to the corresponding authors.

Author contributions

All authors listed have made a substantial, direct, and intellectual contribution to the work and approved it for publication.

Acknowledgments

Conflict of interest

The authors declare that the research was conducted in the absence of any commercial or financial relationships that could be construed as a potential conflict of interest.

Publisher's note

All claims expressed in this article are solely those of the authors and do not necessarily represent those of their affiliated organizations, or those of the publisher, the editors and the reviewers. Any product that may be evaluated in this article, or claim that may be made by its manufacturer, is not guaranteed or endorsed by the publisher.

References

Belaid, S., Rekioua, D., Oubelaid, A., Ziane, D., and Rekioua, T. (2022). A power management control and optimization of a wind turbine with battery storage system. *J. Energy Storage* 45, 103613. doi:10.1016/j.est.2021.103613

Belaid, S., Rekioua, D., Oubelaid, A., Ziane, D., and Rekioua, T. (2022). Proposed hybrid power optimization for wind turbine/battery system. *Periodica Polytech. Electr. Eng. Comput. Sci.* 66 (1), 60–71. doi:10.3311/ppee.18758

Berrueta, A., Soto, A., Marcos, J., de la Parra, Í., Sanchis, P., and Ursúa, A. (2020). Identification of critical parameters for the design of energy management algorithms for li-ion batteries operating in PV power plants. *IEEE Trans. Industry Appl.* 56 (5), 4670–4678. doi:10.1109/tia.2020.3003562

Bragard, M., Soltau, N., De Doncker, R. W., and Schmiegel, A. (2010). Design and implementation of a 5 kW photovoltaic system with li-ion battery and additional DC-DC converter. in 2010 IEEE Energy Conversion Congress and Exposition. Atlanta, GA, USA, 12-16 September 2010, IEEE, 2944–2949.

Campana, P. E., Cioccolanti, L., François, B., Jurasz, J., Zhang, Y., Varini, M., et al. (2021). Li-Ion batteries for peak shaving, price arbitrage, and photovoltaic self-consumption in commercial buildings: A Monte Carlo analysis. *Energy Convers. Manag.* 234, 113889. doi:10.1016/j.enconman.2021.113889

Dashtdar, M., Bajaj, M., and Hosseinimoghadam, S. M. S. (2022). Design of optimal energy management system in a residential microgrid based on smart control. *Smart Sci.* 10 (1), 25–39. doi:10.1080/23080477.2021.1949882

Energy Matters (2020). Kyocera multi-crystal photovoltaic modules. Available at: https://www.energymatters.com.au/images/kyocera/KC200GT.pdf.

Evans, A., Strezov, V., and Evans, T. J. (2009). Assessment of sustainability indicators for renewable energy technologies. *Renew. Sustain. energy Rev.* 13 (5), 1082–1088. doi:10.1016/j.rser.2008.03.008

Fathabadi, H. (2019). Combining a proton exchange membrane fuel cell (PEMFC) stack with a Li-ion battery to supply the power needs of a hybrid electric vehicle. *Renew. energy* 130, 714–724. doi:10.1016/j.renene.2018.06.104

Ferahtia, S., Djerioui, A., Zeghlache, S., and Houari, A. (2020). A hybrid power system based on fuel cell, photovoltaic source and supercapacitor. *SN Appl. Sci.* 2 (5), 940–941. doi:10.1007/s42452-020-2709-0

Ferahtia, S., Djerioui, A., Mesbahi, T., Houari, A., Zeghlache, S., Rezk, H., et al. (2021). Optimal adaptive gain LQR-based energy management strategy for battery–supercapacitor hybrid power system. *Energies* 14 (6), 1660. doi:10.3390/en14061660

Gonzalez, A. A., Bottarini, M., Vechiu, I., Gautier, L., Ollivier, L., and Larre, L. (2019). Model predictive control for the energy management of A hybrid PV/Battery/Fuel cell power plant. In 2019 International Conference on Smart Energy Systems and Technologies (SEST). Porto, Portugal, 9-11 September 2019, 1–6. IEEE. þ

Hannan, M. A., Hoque, M. M., Hussain, A., Yusof, Y., and Ker, P. J. (2018). State-of-the-art and energy management system of lithium-ion batteries in electric vehicle applications: Issues and recommendations. *Ieee Access* 6, 19362–19378. doi:10.1109/access.2018.2817655

Kewat, S., Singh, B., and Hussain, I. (2018). Power management in PV-battery-hydro based stand-alone microgrid. *IET Renew. Power Gener.* 12 (4), 391–398. doi:10.1049/iet-rpg.2017.0566

Khadepaun, N. C., and Shah, N. (2020). Operation of solar PV with PEM fuel cell for remote hybrid microgrid. In 2020 IEEE International Conference on Electronics, Computing and Communication Technologies (CONECCT). Bangalore, India, 02-04 July 2020, IEEE, 1–6.þ

Li, Q., Li, N., Ishida, M., and Zhou, H. (2015). Saving electric energy by integrating a photoelectrode into a Li-ion battery. *J. Mater. Chem. A* 3 (42), 20903–20907. doi:10.1039/c5ta06908d

Mesbahi, T., Rizoug, N., Bartholomeüs, P., Sadoun, R., Khenfri, F., and Le Moigne, P. (2017). Optimal energy management for a li-ion battery/supercapacitor hybrid energy storage system based on a particle swarm optimization incorporating Nelder–Mead simplex approach. *IEEE Trans. Intelligent Veh.* 2 (2), 99–110. doi:10.1109/TIV.2017.2720464

Molina, M. G., and Juanico, L. E. (2010). Dynamic modelling and control design of advanced photovoltaic solar system for distributed generation applications. *J. Electr. Eng. Theory Appl. (JEETA)* 1 (3), 141–150. doi:10.5772/7092

Ongaro, F., Saggini, S., and Mattavelli, P. (2012). Li-ion battery-supercapacitor hybrid storage system for a long lifetime, photovoltaic-based wireless sensor network. *IEEE Trans. Power Electron.* 27 (9), 3944–3952. doi:10.1109/tpel.2012.2189022

Qazi, A., Hussain, F., Rahim, N. A., Hardaker, G., Alghazzawi, D., Shaban, K., et al. (2019). Towards sustainable energy: A systematic review of renewable energy sources, technologies, and public opinions. *IEEE Access* 7, 63837–63851. doi:10.1109/access.2019.2906402

Rezk, H., Aly, M., Al-Dhaifallah, M., and Shoyama, M. (2019). Design and hardware implementation of new adaptive fuzzy logic-based MPPT control method for photovoltaic applications. *Ieee Access* 7, 106427–106438. doi:10.1109/access.2019.2932694

Rizzo, S. A., and Scelba, G. (2015). ANN based MPPT method for rapidly variable shading conditions. *Appl. Energy* 145, 124–132. doi:10.1016/j.apenergy.2015.01.077

Robles Algarín, C., Taborda Giraldo, J., and Rodriguez Alvarez, O. (2017). Fuzzy logic based MPPT controller for a PV system. *Energies* 10 (12), 2036. doi:10.3390/en10122036

Rydh, C. J., and Sandén, B. A. (2005). Energy analysis of batteries in photovoltaic systems. Part I: Performance and energy requirements. *Energy Convers. Manag.* 46 (11-12), 1957–1979. doi:10.1016/j.enconman.2004.10.003

Saleh, A. L., Obed, A. A., Hassoun, Z. A., and Yaqoob, S. J. (2020). Modeling and simulation of A low cost perturb& observe and incremental conductance MPPT techniques. in Proteus Software Based on Flyback Converter" In IOP Conference Series: Materials Science and Engineering, 10 August 2020, Iraq: IOP Publishing, 012152.

Shang, L., Guo, H., and Zhu, W. (2020). An improved MPPT control strategy based on incremental conductance algorithm. *Prot. Control Mod. Power Syst.* 5 (1), 14–18. doi:10.1186/s41601-020-00161-z

Sharma, S., Sood, Y. R., Sharma, N. K., Bajaj, M., Zawbaa, H. M., Turky, R. A., et al. (2022). Modeling and sensitivity analysis of grid-connected hybrid green microgrid system. *Ain Shams Eng. J.* 13 (4), 101679. doi:10.1016/j.asej.2021.101679

Shiau, J. K., Ma, D. M., Yang, P. Y., Wang, G. F., and Gong, J. H. (2009). Design of a solar power management system for an experimental UAV. *IEEE Trans. Aerosp. Electron. Syst.* 45 (4), 1350–1360. doi:10.1109/taes.2009.5310303

Sinsel, S. R., Riemke, R. L., and Hoffmann, V. H. (2020). Challenges and solution technologies for the integration of variable renewable energy sources-a review. *Renew. Energy* 145, 2271–2285. doi:10.1016/j.renene.2019.06.147

Tofighi, A., and Kalantar, M. (2011). Power management of PV/battery hybrid power source via passivity-based control. *Renew. Energy* 36 (9), 2440–2450. doi:10.1016/j.renene.2011.01.029

Vonsien, S., and Madlener, R. (2020). Li-ion battery storage in private households with PV systems: Analyzing the economic impacts of battery aging and pooling. *J. Energy Storage* 29, 101407. doi:10.1016/j.est.2020.101407

Yaqoob, S. J., Hussein, A. R., and Saleh, A. L. (2020). Low cost and simple P&O-MPP tracker using flyback converter. *Solid State Technol.* 63 (6), 9676–9689.

Nomenclature

AC alternating current

CHP combined heat power

DC Direct-current

DG distributed generation units

EMS energy management strategy

EVs electric vehicles

FC Fuel cell

HPS Hybrid power system

IC incremental conductance

LCOE Levelized Cost of Energy

LF Load following

MG Microgrid

MPPT Maximum power point tracking

P&O perturb and observe

PEM proton exchange membrane

PI proportional-integral

PMC power management control

PV photovoltaic

RES renewable energy sources

TNPC Total Net Present Cost

VSS variable step size

WT wind turbine

Abbreviations

I_{pv} PV array currenr (A)

V_{pv} PV array voltage (V)

I_{Ph} the source of the photo (A)

I_o the current of diode at a saturation case (A)

V_A the array's voltage

R_s the series resistance (Ω)

R_{sh} the parallel resistance (Ω)

N_S the total number of panels in a series

N_P the number of parallel panels

γ the constant of the diode

V_{Th} the thermal voltage (V)

N_{ser} the total number cells for one a PV module

T the temperature (℃)

K the constant of Boltzmann $(1.3806503 \times 10^{-23}$ J/°K$)$

q the charge value of the electron $(1.60217646 \times 10^{-19}C)$

V_b the output voltage of the battery (V)

E_0 the voltage at the open-circuit case

Q the normal battery's capacity (Ah)

K the polarization constant

it the current battery charge (Ah)

A_b the exponential zone amplitude (V); B denotes the exponential zonetime constant inverse in the exponential zone (Ah^{-1})

R_b the internal resistance (Ω)

i the battery current

$i^\star$ the filtered current (A)

L inductor current (mH)

C_{in} the input capacitor (μF)

C_{out} the output capacitor (μF)

V_{out} the voltage of the boost converter

ΔV_{out} the volatge's ripple

δ the duty cycle

f_s the switching frequency

ΔI_{pv} the ripple in the input current

y the flat model

x the state variable

u the control variable

$\phi, \varphi,$ **and** ψ the functions of the smooth mapping

$y^{(\beta+1)}$ the notation for the derivative of the output $(\beta + 1)^{th}$

α a finite number of the derivative

C_{bus} the DC bus capacitance

v_{bus} the bus voltage

P_{PVo} the generated power from the PV system

P_{Bato} the generated power from the battery

r_{PV} the PV converter losses

r_{Bat} the battery converter losses

P_{Bat_ref} reference power of the battery

P_{PV_ref} reference power of the PV system (W)

$P_{Bat,max}$ maximum power of the battery (W)

i_{load} current of the load (A)

P_{load} the load power (W)

K_p the proportional gain

K_i the integral gain

ω_n the natural frequency (rad/sec)

ζ the damping factor.